

Exploratory Hand: Leveraging Safe Contact to Facilitate Manipulation in Cluttered Spaces

Michael A. Lin*, Rachel Thomasson*, Gabriela Uribe, Hojung Choi and Mark R. Cutkosky

Abstract—We present a new gripper and exploration approach that uses an exploratory finger with very low reflected inertia for probing and then grasping objects. Equipped with sensing and force control, the finger allows a robot to identify object properties and locations for a secure grasp – without moving very slowly or knocking things over. Employing the finger with robot force/torque and position sensing, the robot can locate contacts using contact normal particle filtering. Adding tactile sensing and finger force control permits approximately 4x faster object localization.

I. INTRODUCTION

Historically, avoiding contact has been synonymous with safety for robotic manipulators. As robots branch out from industrial settings into unstructured environments such as the home, the definition of safety must be expanded. For a robot to help in spaces such as a kitchen, it must be comfortable with contact. Constrained, cluttered spaces place kinematic limitations on a robot’s ability to find and execute collision-free trajectories. Additionally, home settings are characterized by uncertainty, for instance due to occluded vision, which can lead to unexpected contacts. In such settings, contacts can also be leveraged to plan motions [1, 2], reduce uncertainty [3] and perform tasks such as object localization [4] and grasp execution [5, 6]. Therefore, ensuring that contacts, both planned and unplanned, do not lead to unsafe behavior (e.g. damaging, toppling, or excessively displacing objects) will enable robot manipulators to more effectively operate in household spaces.

It is difficult to ensure that incidental contacts are safe through controls alone as collisions happen at a short timescale, often faster than a robot controller’s response time. This is especially true if the robot is moving quickly, which increases the likelihood that dangerous actions will occur. Limiting maximum speed is a common technique for promoting safety, though this is often impractical from a performance standpoint. An alternative approach is to address safety at the mechanical level. Low inertia, highly backdrivable robotic arms have been proven effective for maintaining safe contact when collaborating with humans [7]. In the event of collision, a manipulator with low inertia both imparts smaller impulsive forces and requires less actuator effort to decelerate away from the object it collided

This work was supported in part by the Toyota Research Institute and in part by NSF GRFs for R. Thomasson and M. A. Lin. H. Choi is supported by the Kwanjeong Fellowship.

*These authors contributed equally to this work.

All authors are with the Mechanical Engineering Dept., Stanford University, Stanford, CA 94305, USA (e-mail: mlinyang@stanford.edu)

with, thereby reducing undesirable behavior associated with sustained contact.

In this work, we extend this idea to a low inertia and highly backdrivable end-effector. For manipulation tasks in which contact occurs primarily at the end-effector, the effective inertia of the system is dominated by the inertia of the fingers. As such, a low inertia gripper, even when used with a highly non-backdrivable arm, exhibits a lower effective inertia than a heavy, non-backdrivable gripper used with a low inertia arm. The contributions of this work are:

- 1) A force-controlled, low inertia, backdrivable parallel jaw gripper that can render low impedances without compromising grasp performance.
- 2) Analysis of contact forces during collisions as a function of speed and design parameters of the robot and gripper.
- 3) A fast, contact-based grasp primitive that leverages the gripper’s low inertia and control to quickly acquire objects with position uncertainty.
- 4) An algorithm that uses particle filtering with tactile sensing and perception to localize objects through contact.

These contributions are combined in a demonstration of an exploration task in which the end-effector leverages contact to localize, infer the properties of, and grasp a target object in sparse clutter.

A. Related Work

Grasping under uncertainty: The task of grasping under object state uncertainty can be approached through mechanical design and control. Mechanical solutions include exploiting compliance, kinematics and under-actuation to obtain a large basin of attraction for object acquisition. Notable examples include [3, 8]–[10] and [11] provides an extensive review. However, compliance and under-actuation can also make it more difficult use finger/object contacts to reduce uncertainty on the state of the environment.

In comparison, control approaches combine sensing and actuation to create closed-loop behavior that is robust to uncertainty. Pastor et al. developed a method that corrects movement plans based on tactile feedback [6]. Hsiao et al. used state machine flow to sequentially find a path for the gripper to enclose the object [12]. Murali et al. developed an algorithm to scan for an object based on touch events and generate a grasp candidate based on its belief of the object [13]. For these closed-loop methods, the ability to work with light or fragile objects remains limited by the

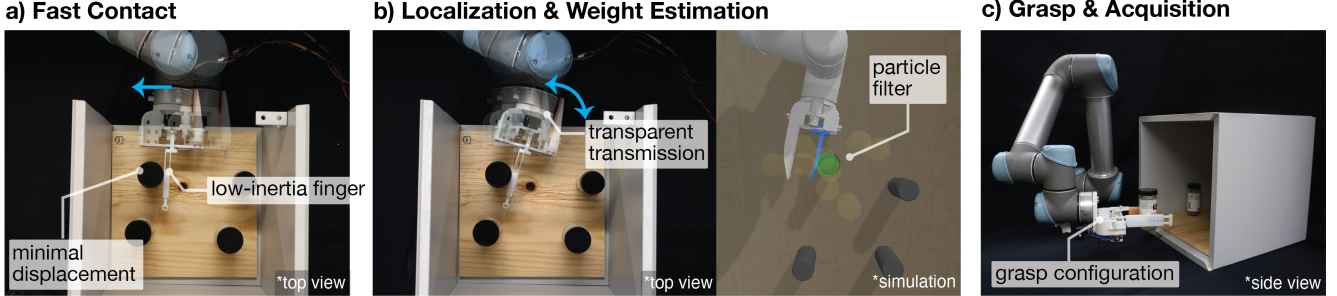


Fig. 1: Exploratory Hand reaches into a constrained space to find and grasp the lightest spice jar. Low inertia and transparent transmission prevent knocking objects over while gathering information about contact locations and object mass. Particle filtering is used to determine contact locations. Finally, the stationary “thumb” is placed adjacent the object and the movable finger grasps it.

mechanical properties of the manipulator and especially the end-effector.

Exploration Through Touch: An additional relevant background area concerns gathering information about the environment through touch. This includes both external properties such as object shape, pose, and surface material, and internal properties such as weight and center of mass. Yi et al. developed a method of determining favorable probe locations for inferring object shape [14]. Petroskaya developed a particle filtering algorithm that is able to determine 6D pose of known objects to millimeter accuracy based on a set of probed points [4]. A more detailed review of techniques for tactile recognition of external object properties can be found in [15]. While external properties can be ascertained by simply touching the surface of objects, internal properties require the robot to manipulate the object to some degree [16].

In general, a challenge of perception through touch is that it may require many contacts, each of which could be costly in terms of time or safe execution. To address this concern, others have investigated proximity sensing for exploration [5, 17], but such sensors are affected by object surface properties [5]. In nature, many animals use whiskers to safely touch, locate, and explore objects with precision [18], and researchers have adapted such strategies to robots (e.g [19, 20]). However, whiskers cannot sense internal object properties as they cannot manipulate. In this work, we present an end-effector with an exploratory finger that is very lightweight so as not to disturb objects, similar to a whisker, but is capable of manipulation. We hypothesise that this combination will reduce the cost of making contact, making tactile exploration more practical in cluttered environments.

Low Inertia Manipulators: Various papers have considered reducing the weight of a robot arm to minimize forces in the event of a collision during collaboration with a human [21, 22]. Others have designed robotic systems that use torque sensing to detect collisions and react via controls. However, controllers cannot react instantaneously, leaving a short amount of time in which impact forces remain high [23]. [7] provides a review of methods for safe human-

robot collaboration. When considering manipulators in the home, the safety of both contact with humans and contact with smaller, lighter household objects should be considered. In the latter case, the impact forces felt by objects before controllers can react may lead to significant unsafe motion. This motivates the choice to use a low inertia design, rather than relying purely on controls for safety. Bhatia et al. presented a robot gripper design with low inertia [24] following similar design principles as those used in legged robots [25]. The gripper presented in [24] operates within a similar design space to the end-effector presented in this work, though the gripper here is kinematically simpler and includes additional design features to maintain high enough grasp forces for a wide range of kitchen items. We also build on top of this work by exploring how this gripper design paradigm can facilitate grasping and exploration in unstructured, cluttered environments.

II. TECHNICAL APPROACH

In the following sections we present details of our gripper design. We then show through experiments that the low inertia and force-transparent transmission can be used for grasping objects based on contact (grasp motion primitive) and 2D localization of objects based on multiple contacts.

A. Gripper Design

The gripper design combines attributes of parallel jaw grippers and low-impedance haptic feedback devices. Parallel jaw grippers are commonly used in industry and research because they are simple to operate, capable of applying large clamping forces, and able to hold objects in a precise position and orientation. To achieve high sustained grasp forces, the transmission typically has a high gear reduction, which makes it challenging to achieve rapid control of grasp and contact forces. The effective finger inertia is typically dominated by the motor inertia multiplied by the square of the gear reduction [26]. The gripper presented here is in contrast designed like a haptic feedback device, with a low mass finger actuated via a capstan drive with a low transmission ratio.

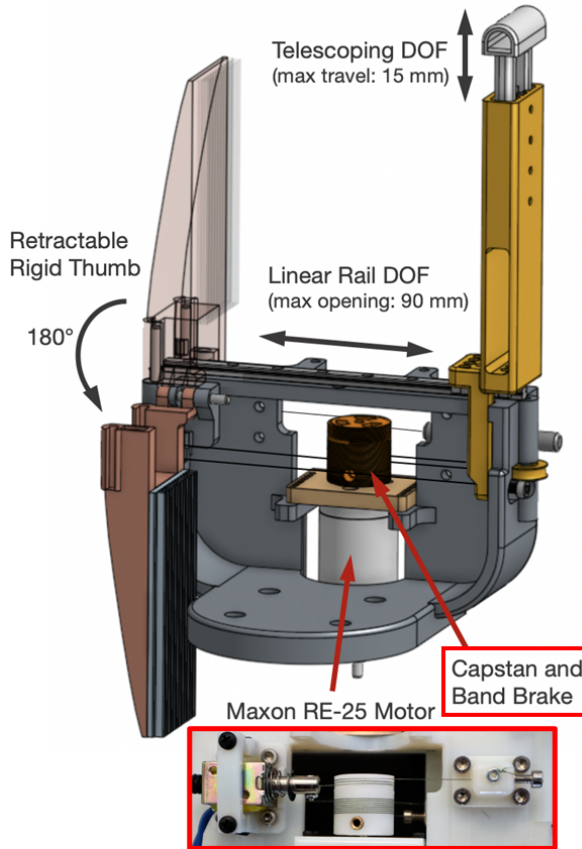


Fig. 2: CAD rendering of gripper with major components and joint limits labeled.

In comparison with tendon-driven linkages, the moving finger has two prismatic degrees of freedom incorporating precise, low friction linear rails. This is so that proprioception can be used to precisely determine object locations through contact sensing. Another consequence of this design is that inertial properties are uniform along the length of the finger, which ensures that contacts at different points along the finger exert similar impact forces.

The mobile finger presses objects against a rigid “thumb” with a high friction surface to provide a precise and secure fixture for them. For transporting heavy objects, it is also possible to rotate the robot wrist so that the weight is borne primarily by the thumb. When probing in an uncertain environment, the thumb can be folded back (see Fig. 2) so that it does not risk bumping objects.

The capstan drive mechanism for the moving finger permits a peak grasp force of 16 N and a sustained force of 11.7 N. As in [27], a solenoid driven band brake is actuated on the capstan to reduce the required motor current when holding heavy objects. In grasp and hold experiments we measured an average of 11.7 N maximum grasping force.

The motor undergoes 10 revolutions over the length of finger travel. This ratio results in an effective mass of:

$$m_{\text{eff}} = m_{\text{link}} + \frac{I_{\text{rotor}} + I_{\text{capstan}}}{r_{\text{capstan}}^2}. \quad (1)$$

The specification of m_{eff} depends on the objects that we will contact (how light and how easily toppled over), and on how fast we want the robot to move. An impulse-momentum calculation provides some initial insight, but the post-contact behavior also depends on assumptions about the robot and how quickly it can decelerate. To explore the range of design parameters for the hand we created a collision model in Working Model 2D (Design Simulation Technologies, Inc.) with assumed robot velocities up to 50 cm/s and a light, tippy object (e.g. a cereal box). The maximum permitted finger inertia to prevent tipping was found for two cases: (i) the finger acted passively after the collision (e.g. under a soft impedance control law) and (ii) a control force rapidly accelerated the finger away from the object after contact. The physical parameters used in the simulation are reported in Table III. The resulting maximum masses were $m_{\text{eff}} = 84$ g and 105 g respectively.

TABLE I: Working Model Analysis Parameters

Coefficients of Static and Dynamic Friction (all bodies)	0.3
Coefficient of Restitution (all bodies)	0.8
Object Width	55 mm
Object Height	260 mm
Object Mass (uniform density)	270 g

The actual effective inertia of the finger is 50.5 g, of which 13.5 g is due to motor and capstan. The second prismatic joint along the finger in the distal direction is passive, with a light spring providing 0.24 lbs/in restoring force. The two prismatic finger joints in combination provide an effective end-point inertia shown in Fig. 4 when mounted to a UR5

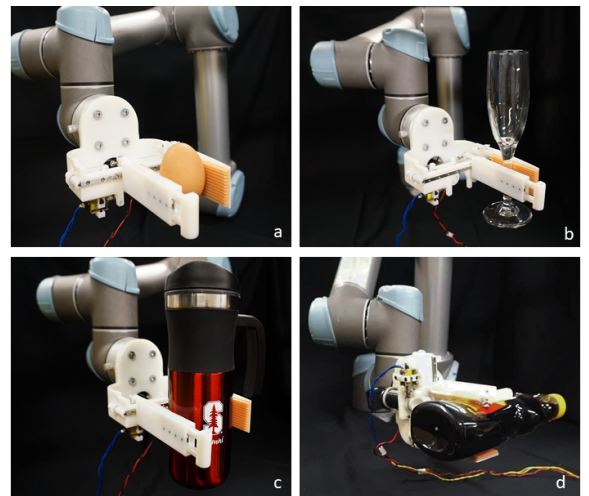


Fig. 3: Exploratory Hand grasping common household objects of different weights and sizes: (a) egg: 56.7 g, (b) champagne flute: 195.2g, (c) coffee mug: 249.2g, (d) maple syrup: 1kg. A non-prehensile grasp is used (d) to carry a heavy object.

robot arm. The computation is preformed as

$$\begin{aligned}\Lambda_v^{-1}(q) &= J_v(q) A^{-1}(q) J_v(q)^T \\ m_{\text{eff}} &= (u^T \Lambda_v^{-1}(q) u)^{-1}\end{aligned}$$

where $J_v(q)$ is the linear Jacobian, $A(q)$ is the inertia matrix, $\Lambda_v(q)$ is the kinetic energy matrix, and u is a unit vector along which the effective mass is being measured. Table II shows the joint angles used for our calculations. We obtained inertia parameters for the UR5 from the manufacturer provided Universal Robot Description File (URDF).¹ For comparison, human fingers have an effective inertia of approximately 6 g [28].

TABLE II: Joint angles used in end-point inertia calculation

J1	J2	J3	J4	J5	J6	J7	J8
0°	-55°	91.6°	-38.4°	90°	180°	0°	0°

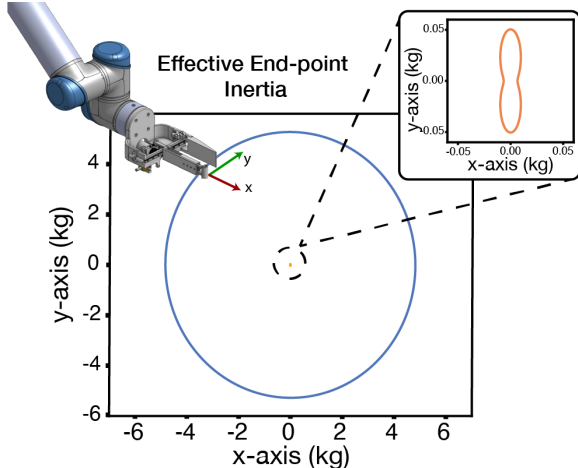


Fig. 4: Effective end-point inertia comparison of UR5 alone vs with Exploratory Hand.

B. System Implementation

The exploratory finger is actuated by a Maxon RE-25 brushed DC motor and controlled with an H-bridge driver and an inline current sensor (Allegro ACS712) for closed-loop current and position control. We use a simple nested control scheme with a PI current controller running at 5 KHz in the inner loop and a PD position controller running at 1 KHz in the outer loop. An embedded microcontroller (Teensy 4.0 Cortex M-7 @600 MHz) is used to execute the controllers and stream position and current sensor data to a computer at 1 KHz via UART. We use Robot Operating System (ROS) to integrate the gripper with a Universal Robot arm (UR5) to perform all experiments.

¹https://github.com/ros-industrial/universal_robot

III. EXPERIMENTS

A. Impact Forces

The goal of this experiment was to examine the impact forces on objects when making unanticipated contact at various speeds. The UR5 robot is commanded to move towards the object at a constant Cartesian velocity and stop when contact is detected. As compared to a system using a standard commercial gripper, we hypothesize that the Exploratory Hand will produce lower forces at higher speeds. Forces are measured by coming into contact with a sensorized peg (using an ATI mini-45 Force/Torque sensor). Measured forces are saturated at approximately 14 N as the peg is designed to separate from the sensor at higher forces to prevent damage.

Four conditions were tested: (a) Robotiq 2F-85 gripper with a Robotiq force/torque sensor (FT300), (b) Robotiq 2F-85 gripper with binary contact sensors, (c) Exploratory Hand with contact sensors and (d) Exploratory Hand with contact sensors and 200 g mass added to the moving finger (to explore the sensitivity to finger mass). For case (a), contact events are detected when the FT sensor measures a force greater than 0.5 N. For the other three cases, an interrupt-driven electrical contact sensor is used to detect contact. The UR-5 robot was commanded to approach the peg at speeds ranging from 1-100 mm/s. For cases (c,d) in this experiment the hand was unpowered.

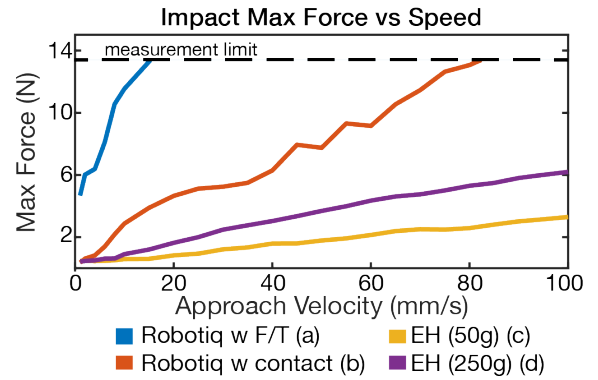


Fig. 5: Plot shows maximum measured force when making contact at different velocities under each condition.

Figure III-A plots maximum impact forces as a function of robot velocity. For case (a), we observed that forces were large even at low speeds, causing our measurement setup to saturate at speeds greater than 10 mm/s. The main factor causing these large forces was the communication latency from the FT sensor (Modbus communication), which was near 30 ms. In practice, other factors that would affect contact detection include gripper inertia, gravity, sensor filtering latencies, etc., which can make it challenging to perform accurate contact detection. In case (b), we abstract away the FT latency issues by using electrical contact sensors, and observe that forces are still relatively large compared to both Exploratory Hand cases. This is due to the much higher effective end-point inertia of the system using the Robotiq

gripper, which results in higher initial impulses and limits the rate at which the robot can decelerate after collision. Cases (c,d) show lower impact forces across all approach velocities, with case (d) producing higher forces, as anticipated, due to the added 200 g finger mass.

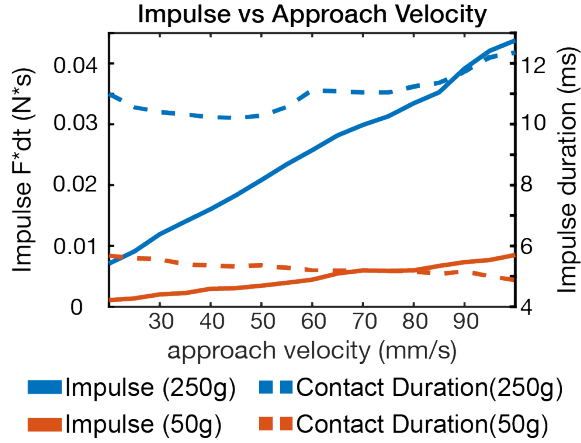


Fig. 6: Plot shows measured impulse when making contact with Exploratory Hand at different velocity. As expected, the impulse for the case with added finger weight (250 g) is 5 times that of the case with no added weight (50 g).

Figure 6 provides another view of the relationship between gripper mass and impact, for the case of the unmodified Exploratory Hand (50 g) and for the hand with 200 g added mass. The impulse duration in this plot is obtained using the electrical contact sensor between the finger and object. As expected, there is an approximately linear relationship between impulse and incoming velocity.

B. Maximum Speed Before Shifting or Toppling Objects

An advantage of maintaining low contact forces is that interactions are less likely to perturb objects, which could increase rather than decrease uncertainty. In cases where pre-existing plans depend on the state of the environment (e.g. path or grasp plans), preserving the object location avoids the need to replan.

To gain additional insight into gripper-object interactions, we performed experiments in which the robot end-effector collides with free-standing objects at various speeds. In two sets of experiments, we measured the maximum contact speed before the object either slipped > 2 mm in the horizontal direction or toppled over. Parameters for the tested objects are provided in Table III. We conducted two sets of experiments: one with contacts at half the object height and one with contacts near the top of the object, with objects resting on a rubber mat so that they were more likely to tip than slide. Two conditions were tested: using a Robotiq gripper on the UR5, or using the Exploratory Hand, with the motor turned off. Contact was detected using the same binary sensors as in the previous experiment. For each condition we conducted 6 trials. For three trials we started at a low speed and increased the speed by 2 mm/s until the object either slipped or toppled. The other three trials started at a high

speed and decremented the speed by 2 mm/s until neither of the failure criteria occurred.

TABLE III: Parameters of objects used for experiments in III-B

Object	Spice Bottle 1	Spice Bottle 2	Cereal box
Width/Diameter	45 mm	45 mm	55 mm
Height	110 mm	110 mm	260 mm
Weight	40 g	220 g	270 g
Material	Plastic	Plastic	Cardboard

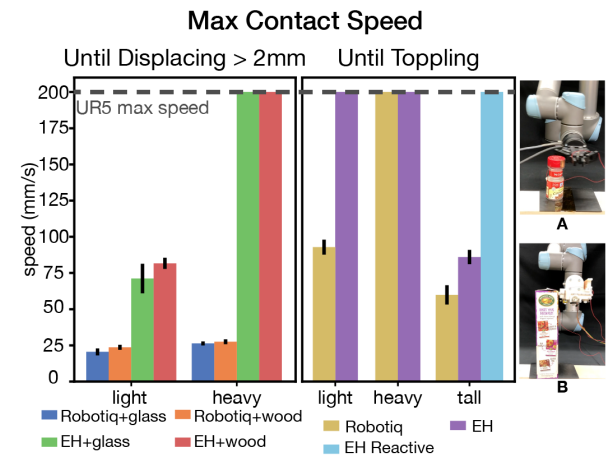


Fig. 7: Left plot shows maximum contact speed before displacing an object > 2 mm; right plot shows maximum speed before toppling objects. Tests conducted with UR5 robot and either Robotiq gripper or Exploratory Hand (EH) with light and heavy objects from Table III, and glass or wood surfaces (left) or a rubber mat (right).

The results of the experiments are summarized in Fig. 7. In the left plot, we observe that for both light and heavy objects, the Exploratory Hand (EH) can approach with substantially higher speeds before slippage occurs. For heavy objects, the speed was limited only by the maximum speed of the UR5 robot. Note also that for the Robotiq condition, the maximum speed for heavy objects is not substantially higher than for light objects.

In the right plot, we examine cases limited by toppling, with contacts occurring near the top of the object. Again, for the exploratory hand we were limited by the maximum speed of the UR5 robot for all but the tallest object.

The right plot also shows a cyan bar for a case labeled, “EH Reactive.” In this case we applied maximum current to the finger motor (bang-bang control) to move it away from the object when contact was detected using the contact sensor. With this action we were again able to make contact with the tall object (cereal box) at speeds limited only by the UR5 robot, whereas the “EH” case would topple this tall object at an average speed of 86 mm/s.

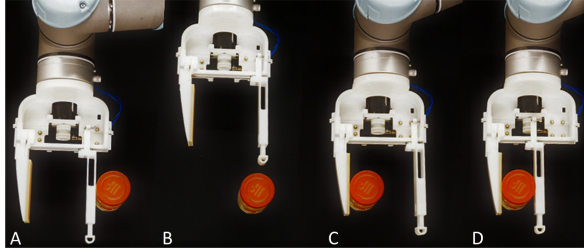


Fig. 8: Contact-based grasp primitive execution begins by approaching an object until making contact with the exploratory finger (A). The contact location is recorded and a motion plan is executed to move around the object (B), placing the rigid thumb at the contact point (C). The exploratory finger closes to complete the grasp (D).

C. Contact-Based Grasp Primitive

The ability to make contact without negative outcomes enables exploration approaches that leverage contact to extract information. For instance, contact information can be used to grasp objects with position uncertainty. We developed a simple grasp primitive that is able to quickly acquire objects based on an initial contact event. The execution (illustrated in Fig. 8) begins by commanding the robot to move at a constant speed toward the expected location of an object such that the back side of the low inertia finger will make initial contact. Upon detecting contact, the location of contact is captured and a sequence of end-effector motions is executed to bring the rigid finger of the gripper in contact with the recorded contact location. Finally, the low inertia finger is commanded to close rapidly and exert a desired grasp force. An advantage of this grasp primitive is that closing the low inertia finger causes little shifting in the location of the object, since the rigid finger is already in contact with the opposite face. Not shifting the object is advantageous because it reduces the chance of ejecting or breaking the object during acquisition. This is due to the object’s non-centered position in the grasp (as opposed to grasping with traditional parallel jaw grippers) and to high certainty regarding the object state post acquisition. Moreover, the entire sequence can be executed at high speeds due to very low inertia of the active finger.

We verified the performance of the grasp primitive in an experiment where a 141 g spice bottle was manually placed at various locations on a wood surface. The location of the object across trials was determined by a grid pattern where the center of the grid is the “expected location,” and adjacent placements were spaced every 2 cm. The grasp primitive was executed 5 times per object placement. Not surprisingly, we found that as long as the object location in the direction along the finger was such that the object was within the length of the finger, the grasp would succeed every time. Of the successful trials, the object was shifted an average of 0.83 mm from its initial pose. Grasps were executed in 1.74 seconds on average after initial contact.

D. Contact-Based Object Localization

Another application of the Exploratory Hand is object localization based on contact information. Due to its low inertia, precise movement, and accurate force control the finger can touch and stay in contact with objects without displacing them as the end-effector pose changes. As a result, we can move the gripper to different poses causing the contact location to roll along the finger and object (see Fig. 9). This action provides us with sequences of contact location observations that can be used to estimate the position of the object given its shape.

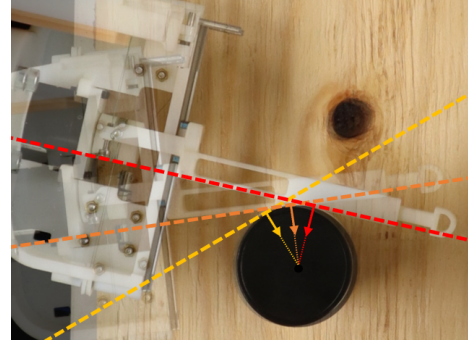


Fig. 9: Rolling motion of the contact during object pose estimation to gather contact information at different orientations.

We implemented a standard particle filtering algorithm to localize the 2D position of an object. As we expect robot-object interactions to cause negligible change in the object location, the dynamics update is just an identity function. The measurement model uses proprioception measurements (joint positions) at each time-step to update the location of the particles. A distance function is used to weight the particles, but since we don’t know where along the finger an object is making contact, the distance metric is projected to the normal direction of the finger:

$$s_i = \hat{u}_n \cdot \vec{d}_i$$

$$p_i = e^{\frac{-|s_i|^2}{2\sigma^2}}$$

where \hat{u}_n is the unit vector normal to the finger, \vec{d}_i is the distance vector from the finger reference frame to each particle location, and σ is the standard deviation that models noise in the measurement. In our case, because contact information is very precise, our σ value can be very low. We only perform observation updates when we detect that the finger is in contact with an object.

To test the localization method, we place a spice bottle at a known location in the robot workspace, execute an end-effector trajectory to make contact, and then rotate about the center of the finger tracking a sine function of 0.2 radians amplitude (shown in the bottom plot of Fig. 10). We used N=200 particles, and assumed an arbitrary prior normal distribution of the object location with a mean that was 15 cm away from the ground truth and a standard deviation of 5 cm. Observation updates were performed at 1 KHz, but called only when the finger was in contact with the object.

Results of the position estimate are shown in Fig. 10. Using proprioception alone we were able to converge to within 1.3 mm from the ground truth location.

Using proprioception to estimate object positions is useful because it is a sensing modality that is available in most robot systems, however, location estimates may converge slowly in the direction along the finger. To improve convergence we included a contact sensor array on the finger surface that detects binary contacts at discrete locations (five 10 mm wide taxels separated by 1 mm gaps) along the finger. We investigated two methods of integrating these sensors: (i) using the measurements on every update step during contact or (ii) using tactile measurements to seed the initial location of the particles and use proprioception thereafter. One challenge for the first method is that the noise introduced by the taxel discretization was much larger than the noise of the proprioception measurements. This prevented the estimates from converging to low errors. To account for the larger noise we combined the taxel and proprioception measurements with separate σ values as follows:

$$s_{n,i} = \hat{u}_n \cdot \vec{d}_i \quad s_{t,i} = \hat{u}_t \cdot \vec{d}_i \\ p_i = e^{\frac{-|s_{n,i}|^2}{2\sigma_n^2} + \frac{-|s_{t,i}|^2}{2\sigma_t^2}}$$

where \hat{u}_n is the same as in the proprioception-only case, \hat{u}_t is the unit vector in the direction along the fingers, σ_n is the standard deviation for the proprioception measurements and σ_t is the standard deviation for the contact array measurements (in our implementation we used $\sigma_n=1$ mm and $\sigma_t=5$ mm). For method (ii) we used a normal distribution with mean at the center of the active taxel and standard deviation of 1 mm. We refer to this method as “hybrid” in Fig. 10, which also shows the convergence of the proprioceptive method (i) and the purely tactile method (ii). For this experiment the final error was 1.3 mm for contact tactile sensing, 1.7 mm for proprioception alone, and 0.8 mm for the hybrid approach.

E. System Demonstration

To illustrate how the Exploratory Hand can be used in real-world settings, we performed a system demonstration, illustrated in Fig. 1, in which the hand identifies and acquires the lightest object from a sparsely cluttered cabinet. First, the exploratory finger sweeps the space until making fast but safe contact with an object, the exact position of which is unknown. The location of the object is then determined using the particle filtering algorithm presented in Section III-D. To determine the relative weight of the objects, the exploratory finger performs a small push of the object and records the force required for displacement. Once this process is repeated for all objects in the scene, the object of the desired relative weight is grasped using knowledge of its location from the exploratory phase.

The main failure case observed in demonstrations is when the rigid palm collides with objects in the environment, introducing uncertainty that could lead to failure of the final grasp. This danger is present when reaching into deep spaces

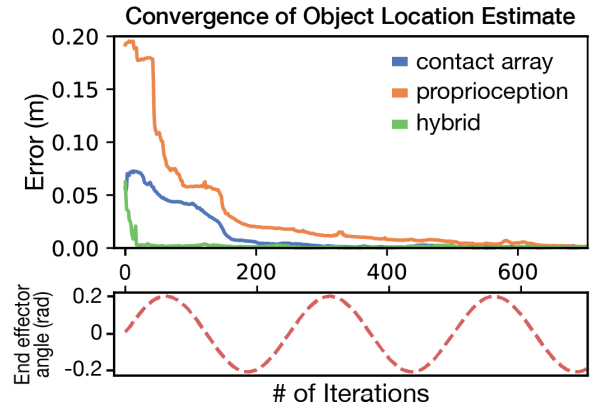


Fig. 10: Contact-based object localization using proprioceptive information alone, a binary contact array, and a hybrid approach with initial contact sensing used to seed the proprioceptive approach. Lower plot shows the commanded gripper oscillation.

where clutter consists of multiple rows of objects. Likelihood of failure was highly impacted by the initial choice of object locations.

IV. CONCLUSIONS AND FUTURE WORK

We have investigated the benefits of a precise, low-inertia gripper with a transmission that is back-driveable and enables accurate force control for exploration in cluttered environments. We show that reducing the effective inertia of the end-effector below a threshold, which depends on the mass of expected objects, enables movement at relatively high speeds in cluttered environments, without danger of substantially perturbing objects. By mitigating the negative consequences of impact, we enable techniques that leverage contact to gain information about the environment. A contact-based grasp primitive is presented for quickly and reliably acquiring objects with positional uncertainty. Additionally, a particle filtering-based object localization algorithm combines tactile and proprioceptive data to quickly converge to a precise estimate of object placement. To show the potential of this new Exploratory Hand for use in real cluttered environments, these techniques are combined for the task of identifying, locating, and acquiring a target object in a cabinet.

As noted in the previous section, an occasional failure case for the cabinet scenario is that the palm of the hand would strike objects first. In the future, controlled pushing motions, as in [29], could be used to rearrange objects toward the front to enable exploration of objects further back. We plan to incorporate additional sensors in future iterations, including contact sensors on non-grasping surfaces such as the palm and a linear encoder for the passive telescoping joint so that it can be used for proprioception. Moreover, we will explore new designs of the exploratory finger that include multiple actuated joints, enabling more reactivity to sensor readings. Integrating multiple sensing modalities can be highly beneficial in complex environments like the home.

Future work will investigate combining the touch-based techniques presented here with vision-based techniques to enable more accurate perception of the environment and allow for execution of higher level tasks in a home setting.

ACKNOWLEDGEMENTS

The authors thank Adithya Murali, Arul Suresh, Samuel Frishman and Alexander Gruebele, for very helpful discussions along the way. Toyota Research Institute (“TRI”) provided funds to assist the authors with their research but this article solely reflects the opinions and conclusions of its authors and not TRI or any other Toyota entity.

REFERENCES

- [1] Advait Jain, Marc D Killpack, Aaron Edsinger, and Charles C Kemp. Reaching in clutter with whole-arm tactile sensing. *The International Journal of Robotics Research*, 32(4):458–482, 2013.
- [2] Mark Moll, Lydia Kavraki, Jan Rosell, et al. Randomized physics-based motion planning for grasping in cluttered and uncertain environments. *IEEE Robotics and Automation Letters*, 3(2):712–719, 2017.
- [3] Clemens Eppner, Raphael Deimel, José Alvarez-Ruiz, Marianne Maertens, and Oliver Brock. Exploitation of environmental constraints in human and robotic grasping. *The International Journal of Robotics Research*, 34(7):1021–1038, 2015.
- [4] Anna Petrovskaya and Oussama Khatib. Global localization of objects via touch. *IEEE Transactions on Robotics*, 27(3):569–585, 2011.
- [5] Kaijen Hsiao, Paul Nangeroni, Manfred Huber, Ashutosh Saxena, and Andrew Y Ng. Reactive grasping using optical proximity sensors. In *2009 IEEE International Conference on Robotics and Automation*, pages 2098–2105. IEEE, 2009.
- [6] Peter Pastor, Ludovic Righetti, Mrinal Kalakrishnan, and Stefan Schaal. Online movement adaptation based on previous sensor experiences. In *2011 IEEE/RSJ International Conference on Intelligent Robots and Systems*, pages 365–371. IEEE, 2011.
- [7] Sandra Robla-Gómez, Víctor M Becerra, José Ramón Llata, Esther González-Sarabia, Carlos Torre-Ferrero, and Juan Pérez-Oria. Working together: A review on safe human-robot collaboration in industrial environments. *IEEE Access*, 5:26754–26773, 2017.
- [8] Zhongkui Wang, Yuuki Torigoe, and Shinichi Hirai. A prestressed soft gripper: design, modeling, fabrication, and tests for food handling. *IEEE Robotics and Automation Letters*, 2(4):1909–1916, 2017.
- [9] Manuel G Catalano, Giorgio Grioli, Edoardo Farnioli, Alessandro Serio, Cristina Piazza, and Antonio Bicchi. Adaptive synergies for the design and control of the pisa/iit softhand. *The International Journal of Robotics Research*, 33(5):768–782, 2014.
- [10] Aaron M Dollar and Robert D Howe. The highly adaptive sdm hand: Design and performance evaluation. *The International Journal of Robotics Research*, 29(5):585–597, 2010.
- [11] C Piazza, G Grioli, MG Catalano, and A Bicchi. A century of robotic hands. *Annual Review of Control, Robotics, and Autonomous Systems*, 2:1–32, 2019.
- [12] Kaijen Hsiao, Sachin Chitta, Matei Ciocarlie, and E Gil Jones. Contact-reactive grasping of objects with partial shape information. In *2010 IEEE/RSJ International Conference on Intelligent Robots and Systems*, pages 1228–1235. IEEE, 2010.
- [13] Adithyavairavan Murali, Yin Li, Dhiraj Gandhi, and Abhinav Gupta. Learning to grasp without seeing. In *International Symposium on Experimental Robotics*, pages 375–386. Springer, 2018.
- [14] Zhengkun Yi, Roberto Calandra, Filipe Veiga, Herke van Hoof, Tucker Hermans, Yilei Zhang, and Jan Peters. Active tactile object exploration with gaussian processes. In *2016 IEEE/RSJ International Conference on Intelligent Robots and Systems (IROS)*, pages 4925–4930. IEEE, 2016.
- [15] Shan Luo, Joao Bimbo, Ravinder Dahiya, and Hongbin Liu. Robotic tactile perception of object properties: A review. *Mechatronics*, 48:54–67, 2017.
- [16] Oleg O Sushkov and Claude Sammut. Active robot learning of object properties. In *2012 IEEE/RSJ International Conference on Intelligent Robots and Systems*, pages 2621–2628. IEEE, 2012.
- [17] Thomas Schlegl, Torsten Kröger, Andre Gaschler, Oussama Khatib, and Hubert Zangl. Virtual whiskers—highly responsive robot collision avoidance. In *2013 IEEE/RSJ International Conference on Intelligent Robots and Systems*, pages 5373–5379. IEEE, 2013.
- [18] Lorenz Pammier, Daniel H O’Connor, S Andrew Hires, Nathan G Clack, Daniel Huber, Eugene W Myers, and Karel Svoboda. The mechanical variables underlying object localization along the axis of the whisker. *Journal of Neuroscience*, 33(16):6726–6741, 2013.
- [19] Joseph H Solomon and Mitra JZ Hartmann. Artificial whiskers suitable for array implementation: accounting for lateral slip and surface friction. *IEEE Transactions on Robotics*, 24(5):1157–1167, 2008.
- [20] Martin J Pearson, Anthony G Pipe, Chris Melhuish, Ben Mitchinson, and Tony J Prescott. Whiskerbot: A robotic active touch system modeled on the rat whisker sensory system. *Adaptive Behavior*, 15(3):223–240, 2007.
- [21] Yong-Jae Kim. Design of low inertia manipulator with high stiffness and strength using tension amplifying mechanisms. In *2015 IEEE/RSJ International Conference on Intelligent Robots and Systems (IROS)*, pages 5850–5856. IEEE, 2015.
- [22] Michael Zinn, Bernard Roth, Oussama Khatib, and J Kenneth Salisbury. A new actuation approach for human friendly robot design. *The international journal of robotics research*, 23(4-5):379–398, 2004.
- [23] Alessandro De Luca, Alin Albu-Schaffer, Sami Haddadin, and Gerd Hirzinger. Collision detection and safe reaction with the dlr-iii lightweight manipulator arm. In *2006 IEEE/RSJ International Conference on Intelligent Robots and Systems*, pages 1623–1630. IEEE, 2006.
- [24] Ankit Bhatia, Aaron M Johnson, and Matthew T Mason. Direct drive hands: Force-motion transparency in gripper design. In *Robotics: Science and Systems*, 2019.
- [25] Gavin Kenneally, Avik De, and Daniel E Koditschek. Design principles for a family of direct-drive legged robots. *IEEE Robotics and Automation Letters*, 1(2):900–907, 2016.
- [26] Kenneth A Pasch and WP Seering. On the drive systems for high-performance machines. 1984.
- [27] Alexa F Siu, Mike Sinclair, Robert Kovacs, Eyal Ofek, Christian Holz, and Edward Cutrell. Virtual reality without vision: A haptic and auditory white cane to navigate complex virtual worlds. In *Proceedings of the 2020 CHI Conference on Human Factors in Computing Systems*, pages 1–13, 2020.
- [28] A. Z. Hajian and R. D. Howe. Identification of the Mechanical Impedance at the Human Finger Tip. *Journal of Biomechanical Engineering*, 119(1):109–114, 02 1997.
- [29] Mehmet R Dogar and Siddhartha S Srinivasa. A planning framework for non-prehensile manipulation under clutter and uncertainty. *Autonomous Robots*, 33(3):217–236, 2012.